

Spin entangled two-particle dark state in quantum transport through coupled quantum dots

Christina Pörtl,^{*} Clive Emary, and Tobias Brandes

Institut für Theoretische Physik, Hardenbergstr. 36, TU Berlin, D-10623 Berlin, Germany

(Dated: September 6, 2012)

We present a transport setup of coupled quantum dots that enables the creation of spatially separated spin-entangled two-electron dark states. We prove the existence of an entangled transport dark state by investigating the system Hamiltonian without coupling to the electronic reservoirs. In the transport regime the entangled dark state which corresponds to a singlet has a strongly enhanced Fano factor compared to the dark state which corresponds to a mixture of the triplet states. Furthermore we calculate the concurrence of the occupying electrons to show the degree of entanglement in the transport regime.

PACS numbers: 03.65.Ud, 73.23.Hk, 73.63.Kv, 85.35.Ds

I. INTRODUCTION

The investigation of dark states (DS) has a long-standing tradition in quantum optics both experimentally¹ and theoretically^{2,3}. In recent years there have been numerous approaches to translate this quantum optical phenomenon into electronic transport^{4–13}. Here, the term DS is used when the current-carrying particles, in general electrons, are trapped in a coherent superposition of states that is decoupled from the collector. The particle flow through the system is blocked, as no further electrons can enter the system due to the Coulomb blockade (CB). The first concepts used similar system setups as in quantum optics and included interactions with microwaves in order to create the DS^{4,5}.

A triple quantum dot (TQD) with a single excess electron was the first system where an *all-electronic* DS was found by Michaelis *et al.*^{7,8}. Hence, the system is driven into the DS purely due to the coupling to the electronic reservoirs. Michaelis *et al.* showed the coherent trapping effect in the TQD and its destabilization due to charge fluctuations. This electronic DS was found to give rise to an enhanced Fano factor⁸ above the Poissonian value $F > 1$. The influence of a magnetic field on the DS formation in the TQD was studied in Ref. [9,11] and Weymann *et al.*¹⁴ have presented the effects of co-tunneling on the DS formation. The influence of phonon interaction on the dark state formation in the TQD was studied in Ref. [15], and Ref. [16] showed how the TQD dark state can be used as a nanomechanical resonator cooler.

We have previously shown¹⁷ that transport DS are not solely an issue of strong Coulomb blockade systems with only a single excess electron. In a TQD with a second excess electron, a two-electron DS can be found for certain configurations. This two-electron DS can also be used as nanomechanical resonator cooler¹⁸. That electronic DSs also occur in interaction with other blockade phenomena is shown in Ref. [10] where a mixture of a spin blockade and a single-electron DS was shown to lead to a quasi two-electron DS.

While the two-electron DS in the single TQD of Ref. [17] is a product state of two single-electron DSs, in this paper we introduce a system that enables the preparation of a spin-entangled two-electron DS. For this aim, we consider two triple quantum dots with a single excess electron in each dot. A possible application of this setup is the creation of spacial separated entangled electrons on demand.

The structure of this article is the following: After introducing the model in Sec. II, we investigate the existence of dark states in the closed system without coupling to the electronic reservoirs in Sec. III. The transport properties, namely stationary current and Fano factor, are discussed in Sec. IV and in order to show the degree of entanglement in the transport regime we calculate the concurrence in Sec. V.

II. MODEL

Fig. 1 shows two possible configurations of the two TQDs. Both TQDs are in the strong Coulomb blockade regime. Such that, up to one electron is allowed in each TQD. The TQDs are close together therefore we have a finite charging energy between the TQDs. Furthermore, we introduce an isotropic exchange interaction acting between the two TQDs. The complete closed system Hamiltonian \hat{H}_D is given by

$$\hat{H}_D = \hat{H}_{\text{TQD},a} + \hat{H}_{\text{TQD},b} + \hat{U} + \hat{J}, \quad (1)$$

where the TQD Hamiltonians are given by

$$\hat{H}_{\text{TQD},A} = \sum_{i=1}^3 \sum_{\sigma} E_{i,A} \hat{n}_{i\sigma,A} + T_A \sum_{j=1}^2 \sum_{\sigma} (d_{j\sigma,A}^{\dagger} d_{3\sigma,A} + h.c.), \quad (2)$$

with $A \in \{a, b\}$, $d_{i\sigma,A}$ is the annihilation operator, and $\hat{n}_{i\sigma,A}$ is the corresponding number operator of an electron in quantum dot (QD) i of TQD A with spin σ . We assume spin-independent energy levels and denote the energy of the single-electron level of a quantum dot QDi,A

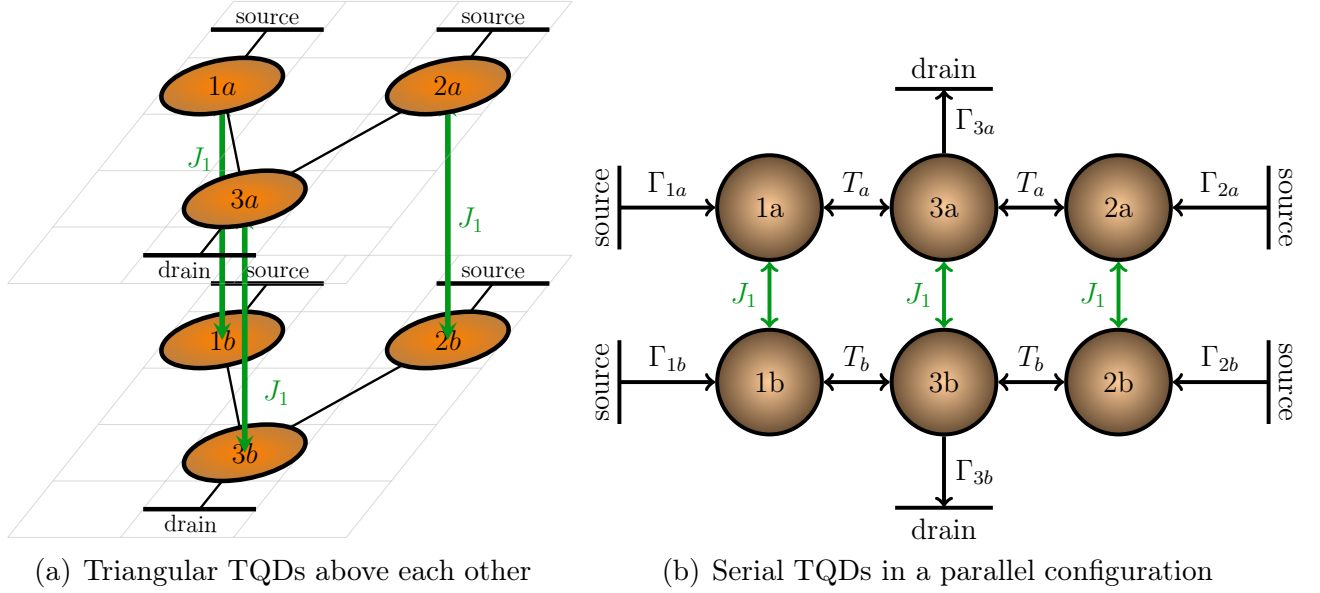


Figure 1: Both TQDs are in the strong Coulomb blockade regime such that up to one electron is allowed in each TQD. The electrons in the TQDs interact with each other capacitively due to the charging energies U_{ij} and due to the exchange interaction switching the spins of the electrons. (The exchange interaction J_1 is indicated in the sketches). Each TQD is connected to two sources and one drain. Here, two possible configurations are shown (a) where the two TQDs are triangular and lie above each other and (b) where the TQDs are serial and parallel to each other. In configuration (a) the special distance between QD1 and QD2 is smaller than in configuration (b), therefore the effects of decoherence which may destroy the DS in this configuration are smaller.

as $E_{i,A}$. In the following we set all $E_{i,A} = 0$. The levels in QD1,A and QD2,A are coupled coherently to QD3,A with a tunnel amplitude T_A . The charging energy is the capacitive part of the Coulomb interaction and given by

$$\hat{U} = \sum_{i,j} \sum_{\sigma,\sigma'} U_{ij} \hat{n}_{i\sigma,a} \hat{n}_{j\sigma',b}, \quad (3)$$

where U_{ij} is the additional charging energy needed to add an electron to QD i of TQD a when QD j of TQD b is occupied with one electron. In this setup an electron in TQD a always interacts with an electron in TQD b , as both TQDs are in the strong Coulomb blockade. Therefore terms for having two electron in a single TQD are not included \hat{U} , as they are assumed to far above the transport window and not relevant for the transport.

The isotropic exchange energy is

$$\begin{aligned} \hat{J} &= \sum_{i,j} J_{ij} (\sigma_{i,a} \cdot \sigma_{j,b}) = \sum_{i,j} J_{ij} (\sigma_{i,a}^x \sigma_{j,b}^x + \sigma_{i,a}^y \sigma_{j,b}^y + \sigma_{i,a}^z \sigma_{j,b}^z) \\ &= \sum_{i,j} J_{ij} (\sigma_{i,a}^z \sigma_{j,b}^z + 2(\sigma_{i,a}^+ \sigma_{j,b}^- + \sigma_{i,a}^- \sigma_{j,b}^+)) \\ &= \sum_{i,j} J_{ij} [(\hat{n}_{i\uparrow,a} - \hat{n}_{i\downarrow,a})(\hat{n}_{i\uparrow,b} - \hat{n}_{i\downarrow,b}) \\ &\quad + 2(d_{i\uparrow,a}^\dagger d_{i\downarrow,a} d_{j\downarrow,b}^\dagger d_{j\uparrow,b} + d_{i\downarrow,a}^\dagger d_{i\uparrow,a} d_{j\uparrow,b}^\dagger d_{j\downarrow,b})], \end{aligned} \quad (4)$$

where the σ are the Pauli-matrices, i and j label the QDs of the TQD a or b and J_{ij} are the exchange constants. In the following we set $J_{ii} = J_1$ and $J_{ij} = J_2$, $i \neq j$. In

this article we treat this exchange interaction as a part of the Coulomb interaction between the electrons.¹⁹ The system Hamiltonian in the localized basis can be found in Appendix A. We will later on refer to the two-electron Hamiltonian blocks $H_{\sigma a \sigma' b}$ for the different spin configuration and the exchange interaction blocks \hat{J} defined in this Appendix.

Each TQD is connected to three electron reservoirs that are described with the Hamiltonian

$$\hat{H}_{\text{res}} = \sum_{\alpha,A} \sum_{k,\sigma} \epsilon_{\alpha k,A} c_{\alpha k \sigma,A}^\dagger c_{\alpha k \sigma,A}, \quad (5)$$

where $\alpha := \{1, 2, 3\}$ labels the reservoirs (1, 2 = source, 3 = drain) and $c_{\alpha k \sigma,A}^\dagger$ is the creation operator of an electron with spin σ in mode k of reservoir α of TQD A . The TQD and the reservoirs are connected by the tunnel Hamiltonian

$$\hat{H}_T = \sum_{\alpha,A} \sum_{k,\sigma} V_{\alpha k,A} c_{\alpha k \sigma,A}^\dagger d_{\alpha \sigma,A} + \text{h.c.} \quad (6)$$

We assume spin-independent reservoir energies $\epsilon_{ik,A}$ and tunneling amplitudes $V_{ik,A}$.

III. CLOSED SYSTEM

The formation of a transport DS $|\Psi_D\rangle$ is only possible if the system Hamiltonian \hat{H}_S fulfills certain conditions.

But the formation of the DS can be destroyed due to decoherence^{4,20} or avoided for special coherent system-bath couplings²⁰, even when these conditions are fulfilled. In the high bias regime^{21,22} all relevant system states lie well within the transport window. Here, a transport DS can be found when the system Hamiltonian block with most excess electrons has an eigenstate $|\Psi_D\rangle$ without finite occupation on the QD(s) which is (are) coupled to the collector(s). For the two-TQD setup this means, we search for an eigenstate in the two electron sector without occupation on QD3 of both TQDs

$$\langle\Psi_D|\hat{n}_{3\sigma,A}|\Psi_D\rangle=0, \quad \forall A,\sigma. \quad (7)$$

In the transport regime such an eigenstate leads in general to a current blockade, where the stationary current of the system drops to zero when the DS becomes occupied.

A. Closed system without exchange interaction

We begin by looking at the system without exchange interaction and set $J_1 = J_2 = 0$, such that the charging energy is the only influence that exists between the two TQDs. Without exchange energy the two-electron sector of the system Hamiltonian consists of four blocks which are uncoupled to each other. Each block corresponds to one of the four possible spin configurations of the occupying electrons. In order to find a transport DS, we are searching for eigenstates without occupation on the third dots in one of these four blocks, hence eigenstates of the form

$$|\Psi_D\rangle = (a_1 d_{1\sigma,a}^\dagger d_{1\sigma',b}^\dagger + a_2 d_{1\sigma,a}^\dagger d_{2\sigma',b}^\dagger + a_3 d_{2\sigma,a}^\dagger d_{1\sigma',b}^\dagger + a_4 d_{2\sigma,a}^\dagger d_{2\sigma',b}^\dagger) |0\rangle, \quad (8)$$

with $|a_1|^2 + |a_2|^2 + |a_3|^2 + |a_4|^2 = 1$. But these blocks are 9×9 matrices and it is in general not possible to calculate all eigenstate analytically, in order to prove that a dark state exists. However, the state $|\Psi_D\rangle$ must fulfill in the spin- $\sigma\sigma'$ sector of the localized basis the condition

$$(H_{\sigma a \sigma' b} - \lambda_D \mathbb{1}) |\Psi_D\rangle = 0. \quad (9)$$

The explicit form of the $H_{\sigma a \sigma' b}$ can be found in Appendix A. Each of these four blocks has equal entries, because we assume spin degenerate single particle energies. Hence, a DS in one of the blocks is degenerated with the DSs at the same energy λ_D in the other three blocks.²³ In the two-TQD setup without exchange interaction we find a DS

$$|\Psi_{D,\sigma\sigma'}\rangle = \frac{1}{2} (d_{1\sigma,a}^\dagger - d_{2\sigma,a}^\dagger) (d_{1\sigma',b}^\dagger - d_{2\sigma',b}^\dagger) |0\rangle, \quad (10)$$

in each block, when the charging energies $U_{12} = U_{11} = U_{22}$ are equal to the DS-eigenenergy $\lambda_D = U_{12}$. The DS of the transport system is then a mixture of the four degenerate states of the closed system.

B. Closed system with exchange interaction

With a finite isotropic exchange interaction the two-electron blocks with opposite spins couple to each other, while the blocks with equal spins remain uncoupled. Now a two-electron DS is found either when

$$\begin{aligned} (H_{\sigma a \sigma b} + \bar{J} - \lambda_D \mathbb{1}) |\Psi_D\rangle &= 0, \quad \text{or} \\ \left(\begin{pmatrix} H_{\uparrow a \downarrow b} - \bar{J} & 2\bar{J} \\ 2\bar{J} & H_{\downarrow a \uparrow b} - \bar{J} \end{pmatrix} - \lambda_D \mathbb{1} \right) |\Psi_D\rangle &= 0, \end{aligned} \quad (11)$$

with

$$\begin{aligned} |\Psi_D\rangle &= (a_1 d_{1\uparrow,a}^\dagger d_{1\downarrow,b}^\dagger + a_2 d_{1\uparrow,a}^\dagger d_{2\downarrow,b}^\dagger + a_3 d_{2\uparrow,a}^\dagger d_{1\downarrow,b}^\dagger \\ &\quad + a_4 d_{2\uparrow,a}^\dagger d_{2\downarrow,b}^\dagger + b_1 d_{1\downarrow,a}^\dagger d_{1\uparrow,b}^\dagger + b_2 d_{1\downarrow,a}^\dagger d_{2\uparrow,b}^\dagger \\ &\quad + b_3 d_{2\downarrow,a}^\dagger d_{1\uparrow,b}^\dagger + b_4 d_{2\downarrow,a}^\dagger d_{2\uparrow,b}^\dagger) |0\rangle, \end{aligned} \quad (12)$$

and $|a_1|^2 + |a_2|^2 + |a_3|^2 + |a_4|^2 + |b_1|^2 + |b_2|^2 + |b_3|^2 + |b_4|^2 = 1$. DSs of the form of Eq. (10) still exist, when the two occupying electrons have equal spin, but now the charging energies have to fulfill the condition $U_{11} = U_{22} = J_2 - J_1 + U_{12}$ and the eigenenergy is shifted to $\lambda_D = J_2 + U_{12}$.

In the opposite spin sector we find now two DS with different condition for the charging energies and with different eigenenergies. For $\lambda_D = -3J_2 + U_{12}$ and $U_{11} = U_{22} = 3J_1 - 3J_2 + U_{12}$ the DS is a singlet state

$$|\Psi_{D,-}\rangle = \frac{1}{\sqrt{2}} (|\Psi_{D,\uparrow\downarrow}\rangle - |\Psi_{D,\downarrow\uparrow}\rangle), \quad (13)$$

and for $\lambda_D = J_2 + U_{12}$ and $U_{11} = U_{22} = J_2 - J_1 + U_{12}$ the DS is a triplet state

$$|\Psi_{D,+}\rangle = \frac{1}{\sqrt{2}} (|\Psi_{D,\uparrow\downarrow}\rangle + |\Psi_{D,\downarrow\uparrow}\rangle). \quad (14)$$

These two dark states are entangled with respect to the spin of the electrons. In the transport regime only the singlet-DS can be prepared as a pure state, since it is not degenerate with any other DSs. The entangled triple-DS Eq. (14) is degenerate with the two DSs in the equal spin sectors, which also correspond to the other two states of the triplet. Not only the degeneracy of the eigenstate is broken, but also the conditions for charging and exchange energies is different for singlet-DS and triplet-DS. This enables to prepare the pure transport singlet-DS in the high bias regime, where all relevant system states are well within the transport window. If the degeneracy is broken, but the condition for the charging energies remains equal for all four DS, it would be only for certain finite transport window configurations possible to prepare the singlet-DS as a pure state.

IV. TRANSPORT PROPERTIES

The considered transport setup is such that all electrons enter the TQDs from the source leads with the

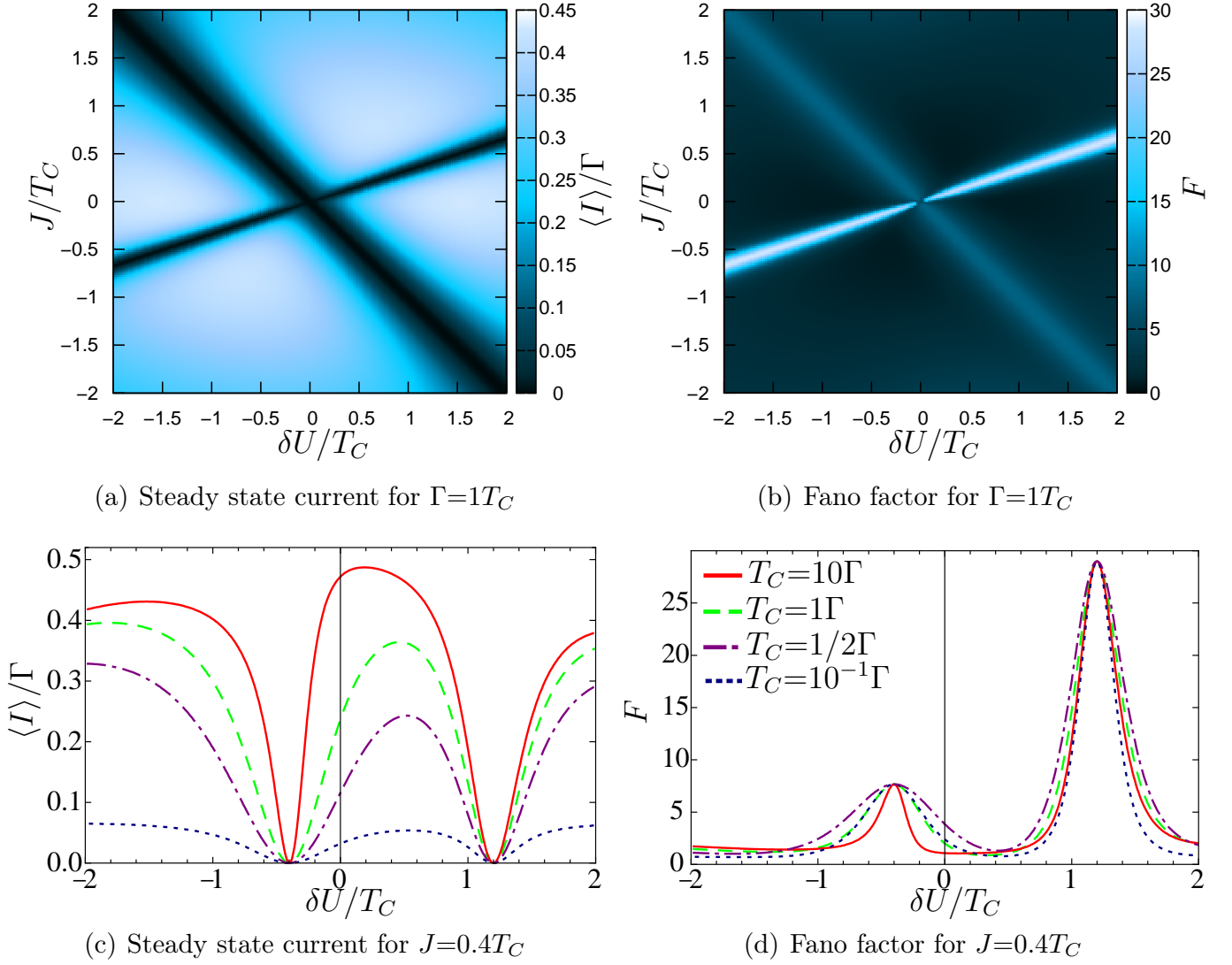


Figure 2: (a) Steady state current $\langle I \rangle / \Gamma$ as a function of the exchange energy J and δU normalized by T_C for $\Gamma / T_C = 1$. The thin dark line (zero current line) in the density plot indicates the formation of the singlet-DS and the thick dark line the formation of the triplet-DS. Fano factor (b) (corresponding to (a)) is highly super-Poissonian around both DSs. But the Fano factor near the singlet-DS is around four times higher than around the triplet-DS. (c) Current as a function of $\delta U / T_C$, for different coupling strength T_C / Γ at $J = 0.4 T_C$. The curve for $T_C = 1 \Gamma$ corresponds to a section through the density plot above. The Fano factors (d) show that the maximum value of the Fano factor near both DS is independent of the ratio T_C / Γ . Parameter: $V = 10 T_C$.

rates Γ_{iA} , $i \in \{1, 2\}$, $A \in \{a, b\}$ depending on the QD and TQD in which the electrons tunnel and leave the TQDs by tunneling into the drain lead with the rate Γ_{3A} . We assume that all considered energy levels of the two TQDs lie well within the transport window. We can therefore use a generalized master equation in Lindblad form^{21,22} to described the transport through the two-TQD setup

$$\dot{\rho} = -i[\hat{H}_D, \rho] + \sum_X \left(D_X \rho D_X^\dagger - \frac{1}{2} D_X^\dagger D_X \rho - \frac{1}{2} \rho D_X^\dagger D_X \right). \quad (15)$$

The explicit form of the 12 coupling terms $X \in \sum_j A \sigma$, with $j \in \{1, 2, 3\}$, $A \in \{a, b\}$, $\sigma \in \{\uparrow, \downarrow\}$, can be found in Appendix B. In order to calculate stationary current and the second-order zero-frequency Fano factor we rewrite Eq. (15) in Liouville space $\dot{\rho}(\chi) = (\mathcal{W}_0 + \mathcal{J}e^{i\chi})\rho(\chi)$ and introduce a counting field^{24–27}. This counting field enables one to introduce the cumulant generating function of the current distribution

$$\mathcal{F}(\chi, t) = \ln \left(\text{Tr}_D \{ e^{(\mathcal{W}_0 + \mathcal{J}e^{i\chi})(t-t_0)} \rho(t_0) \} \right), \quad (16)$$

where $\text{Tr}_D \{ \dots \}$ corresponds to the trace of the density matrix. The n -th order zero frequency current

correlation²⁷ is then evaluated by

$$\langle S^{(n)} \rangle = \frac{d}{dt} \frac{\partial^n}{\partial (i\chi)^n} \mathcal{F}(\chi, t) |_{\chi=0, t \rightarrow \infty}. \quad (17)$$

The second order zero-frequency Fano factor is then defined as

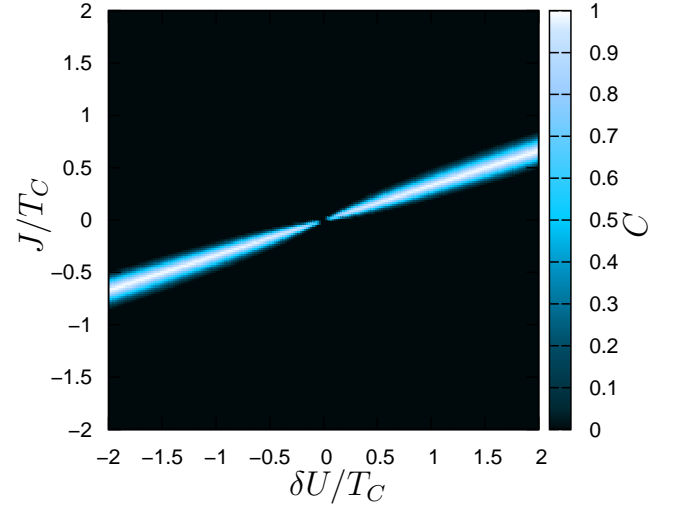
$$F = \frac{\langle S^{(2)} \rangle}{\langle S^{(1)} \rangle}, \quad (18)$$

the 2-th order current correlation functions, normalized by the stationary current ($\langle S^{(1)} \rangle = \langle I \rangle$). Since we are interested in the total current and noise through the system, we count the electrons tunneling from both TQDs. With this the jump operator becomes $\mathcal{J}\rho = \sum_{A,\sigma} D_{3A\sigma} \rho D_{3A\sigma}^\dagger$ and \mathcal{W}_0 correspond to the other terms of the Lindblad equation Eq. (15). We could also count the electrons leaving each TQD separately. However, for the parameter setting, for which we calculate the steady state current and Fano factor in this article, the results would be simply half of the total current and Fano factor.

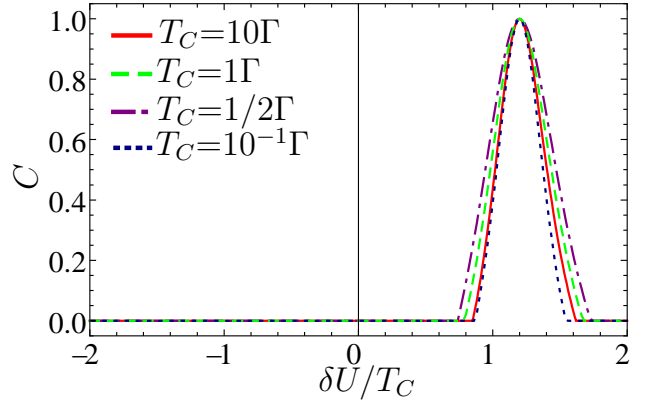
In the following discussion of steady state current and Fano factor we set $J_1 = J$, $J_2 = 0$, $T_a = T_b = T_C$, $\Gamma_{1A} = \Gamma_{2A} = \Gamma_{3A} = \Gamma$, $U_{ii} = U$ and $U_{ij} = V$ for $i \neq j$. We then introduce $\delta U = U - V$ as difference between intra-charging and inter-charging energy. Figure 2 shows total steady state current and Fano factor of the two-TQD setup. Fig. 2(a) is a density plot of the current $\langle I \rangle / \Gamma$ as a function of exchange interaction J and charging energy difference δU normalized by T_C . The formation of both dark states singlet-DS as well as triplet-DS can be seen as dark lines running through the density plot. However, the width of the anti-resonance in the current around the triplet-DS is for this parameter setting much broader than for the singlet-DS. At $\delta U = J = 0$, where the current valleys cross each other, the singlet-DS and the triplet-DSs of the closed system as well as of the transport system live in a degenerated subspace. The transport DS at $\delta U = J = 0$ is therefore a mixture of the three triplet-DS and the singlet-DS.²⁸ Fig. 2(b) shows the according Fano factor to the current density plot. Although the Fano factor reaches near both dark states highly super-Poissonian values, the maximum value around the singlet-DS is strongly increased compared to triplet-DS.

Fig. 2(c) shows the current as a function of the charging energy difference $\delta U / \Gamma$, for different ratios of T_C / Γ . The current increases asymptotic with increasing T_C . Hence, the not shown current and Fano factor curves for $T_C = 100\Gamma$ almost coincide with current and Fano factor curves for $T_C = 10\Gamma$. The width of the current valley around the DSs decreases for both DS with increasing T_C , but again remains finite for $T_C \rightarrow \infty$. Apart from that, the valley around triplet-DS decreases stronger than the valley around singlet-DS.

In Fig. 2(d) the corresponding Fano factor to Fig. 2(c) is shown. The maximum value of the Fano factor near both DSs is independent of the ratio T_C / Γ and highly



(a) Concurrence for $T_C = 1\Gamma$



(b) Concurrence for $J = 0.4T_C$

Figure 3: (a) Concurrence as function of the exchange energy J and δU normalized by T_C for $T_C = 1\Gamma$. (b) Concurrence as a function of δU normalized by T_C at $J = 0.4T_C$ for different ratios of T_C / Γ . Parameter: $V = 10T_C$.

super-Poissonian. But the value of the Fano factor around singlet-DS is around four times higher than the value around triplet-DS. Similar features are found by Burkard *et al.* in²⁹. The width of the Fano factor resonance is widest for $T_C = 1/2\Gamma$ and decreases for both smaller and higher values of T_C / Γ , in the shown plot. Therefore, the width of the Fano factor resonance is not simply decreasing for higher values of T_C / Γ as for the corresponding current.

V. CONCURRENCE

Entanglement is a very important aspect of quantum mechanics. It is responsible for the non-locality of quantum mechanics, which can be tested^{30,31} via the violation of the Bell's inequality³². Apart from that, coherences are the foundation of various concepts in quantum

mechanics such as quantum computation^{33,34}, quantum teleportation^{34–36} and quantum cryptography^{34,37}.

A way to measure the entanglement of a mixed state is to calculate its *concurrence*³⁸ C . The concurrence of a two qubit system is define as $C = \max[0, \sqrt{\lambda_1} - \sum_{j=2}^4 \sqrt{\lambda_j}]$, with λ_j being the eigenvalues of $\rho_{2Q}(\sigma_y \otimes \sigma_y) \rho_{2Q}^*(\sigma_y \otimes \sigma_y)$ in decreasing order. Here, ρ_{2Q} is the density matrix of the two qubit system in the localized basis and the σ_y are the according Pauli matrices of the qubits. The spin degree of freedom is entangled in the two-TQD setup. In order to calculate the concurrence with respect to the spin qubits, it is necessary to trace out the QD states of the stationary state ρ_{stat} of Eq. (15) $\rho_{\text{spin}} = \text{Tr}_{\text{QD}}[\rho_{\text{stat}}]$. The two particle sector of ρ_{spin} corresponds then to ρ_{2Q} .³⁹

Fig. 3(a) shows the concurrence as density plot for the same parameters as 2(a). At the pure entangled singlet-DS the concurrence rises to one indicating a maximal entangled states. Around the mixed triplet-DS the concurrence is zero which corresponds to a state without entanglement. Fig. 3(b) shows the concurrence as a function of $\delta U/T_C$ at $J = 0.4T_C$ for different ratios of T_C/Γ . As for the according Fano factor, Fig. 2(d), the concurrence resonance is widest for $T_C = \frac{1}{2}\Gamma$.

VI. CONCLUSIONS

We have shown that the preparation of a spin-entangled two-electron DS is possible. For this aim we have introduced a setup with two TQDs. The isotropic spin-exchange interaction between the occupying electrons lifts the degeneracy of the singlet-DS with the three triplet-DSs and enables the creation of a pure spin-

entangled singlet-DS. The concurrence, which rises to unity at the singlet-DS, proves the existence of the entanglement in the transport regime. Furthermore, the singlet-DS has a strongly enhanced Fano factor compared to the triplet-DS. This signature of the singlet-DS can be used to separate the entangled DS from the non-entangled-DS by measuring the Fano factor.

As the electrons are still localized in the TQDs, this setup enables the creation of spacially separated spin-entangled electrons on demand. Without any further modifications of the device the entangled electrons are simply stored in the two-TQD setup. Switching the chemical potential of the sources leads, such that they also become collectors, enables the usage the entangled electrons outside of the device. Here, the disadvantage is that each electron has two possibilities to tunnel out of the device, namely the two former source leads of the TQD it is occupying. Theoretical this can be easily avoided by switching the tunnel rate of one of the former sources of each TQD to zero e.g. $\Gamma_{2a} = \Gamma_{2b} = 0$. Experimentally it would probably be easier to consider a setup, which has only one source and one drain lead for both bias configurations. This does not change the essential features as the DS formation and the values of Fano factor and concurrence around the DSs.

Acknowledgment

We are grateful to G. Platero and F. Renzoni for helpful discussions. Financial support by DFG projects GRK 1558, DFG BR 1528/7-1, DFG BR 1528/8-1 and SFB 910 is acknowledged.

Appendix A: Hamiltonian

The system Hamiltonian of the two TQDs above each other has a block structure

$$\hat{H}_D = \begin{pmatrix} 0 & 0 & 0 & 0 & 0 & 0 & 0 & 0 & 0 \\ 0 & H_{\uparrow a} & 0 & 0 & 0 & 0 & 0 & 0 & 0 \\ 0 & 0 & H_{\downarrow a} & 0 & 0 & 0 & 0 & 0 & 0 \\ 0 & 0 & 0 & H_{\uparrow b} & 0 & 0 & 0 & 0 & 0 \\ 0 & 0 & 0 & 0 & H_{\downarrow b} & 0 & 0 & 0 & 0 \\ 0 & 0 & 0 & 0 & 0 & H_{\uparrow a \downarrow b} - \bar{J} & 2\bar{J} & 0 & 0 \\ 0 & 0 & 0 & 0 & 0 & 2\bar{J} & H_{\downarrow a \uparrow b} - \bar{J} & 0 & 0 \\ 0 & 0 & 0 & 0 & 0 & 0 & 0 & H_{\uparrow a \uparrow b} + \bar{J} & 0 \\ 0 & 0 & 0 & 0 & 0 & 0 & 0 & 0 & H_{\downarrow a \downarrow b} + \bar{J} \end{pmatrix}, \quad (\text{A1})$$

where the zero in the first diagonal entry denotes the empty state, the next four entries of the form $H_{\sigma A}$ denote the single-particle sectors of the two-TQD system, with $A \in \{a, b\}$ labeling the TQD and $\sigma \in \{\uparrow, \downarrow\}$ labeling the spin of the electron. In the basis $\{|1_{A\sigma}\rangle, |2_{A\sigma}\rangle, |3_{A\sigma}\rangle\}$ these part have the form

$$H_{\sigma A} = \begin{pmatrix} \Delta_A & 0 & T_A \\ 0 & -\Delta_A & T_A \\ T_A & T_A & 0 \end{pmatrix}. \quad (\text{A2})$$

Here, T_A is the coupling term between QD 1 and 2 to QD 3 and $2\Delta_A$ a detuning between the first and the second dot $E_{1,A} = \Delta_A$, $E_{1,A} = -\Delta_A$ and $E_{3,A} = 0$. The last four diagonal terms $H_{\sigma a \sigma' b}$ are two-particle sectors. In the basis

$$\{|1_{a\sigma}1_{b\sigma'}\rangle, |1_{a\sigma}2_{b\sigma'}\rangle, |1_{a\sigma}3_{b\sigma'}\rangle, |2_{a\sigma}2_{b\sigma'}\rangle, |2_{a\sigma}1_{b\sigma'}\rangle, |2_{a\sigma}3_{b\sigma'}\rangle, |3_{a\sigma}3_{b\sigma'}\rangle, |3_{a\sigma}1_{b\sigma'}\rangle, |3_{a\sigma}2_{b\sigma'}\rangle\},$$

the Hamiltonians become

$$H_{\sigma a \sigma' b} = \begin{pmatrix} U_{11}+\Delta_a+\Delta_b & 0 & T_b & 0 & 0 & 0 & 0 & T_a & 0 \\ 0 & U_{12}+\Delta_a-\Delta_b & T_b & 0 & 0 & 0 & 0 & 0 & T_a \\ T_b & 0 & U_{13}+\Delta_a & 0 & 0 & 0 & 0 & 0 & 0 \\ 0 & 0 & 0 & U_{22}-\Delta_a-\Delta_b & 0 & 0 & 0 & 0 & 0 \\ 0 & 0 & 0 & 0 & U_{21}-\Delta_a+\Delta_b & 0 & 0 & 0 & 0 \\ 0 & 0 & 0 & T_b & 0 & U_{23}-\Delta_a & T_a & 0 & 0 \\ 0 & 0 & T_a & 0 & 0 & T_a & U_{33} & T_b & T_b \\ T_a & 0 & 0 & 0 & T_a & 0 & T_b & U_{31}+\Delta_b & 0 \\ 0 & T_a & 0 & T_a & 0 & 0 & 0 & 0 & U_{32}-\Delta_b \end{pmatrix}. \quad (\text{A3})$$

The \bar{J} denotes isotropic exchange energy terms, with

$$\bar{J} = \begin{pmatrix} J_1 & 0 & 0 & 0 & 0 & 0 & 0 & 0 & 0 \\ 0 & J_2 & 0 & 0 & 0 & 0 & 0 & 0 & 0 \\ 0 & 0 & J_2 & 0 & 0 & 0 & 0 & 0 & 0 \\ 0 & 0 & 0 & J_1 & 0 & 0 & 0 & 0 & 0 \\ 0 & 0 & 0 & 0 & J_2 & 0 & 0 & 0 & 0 \\ 0 & 0 & 0 & 0 & 0 & J_2 & 0 & 0 & 0 \\ 0 & 0 & 0 & 0 & 0 & 0 & J_1 & 0 & 0 \\ 0 & 0 & 0 & 0 & 0 & 0 & 0 & J_2 & 0 \\ 0 & 0 & 0 & 0 & 0 & 0 & 0 & 0 & J_2 \end{pmatrix}. \quad (\text{A4})$$

The off-diagonal J terms in the Block structure Hamiltonian switch the spin of the electrons and the diagonal terms change the effective charging energy of the sector.

Appendix B: Coupling terms

We find 12 coupling terms D_X in the Lindblad equation Eq. (15) of the two-TQD setup:

$$\begin{aligned} D_{3a\sigma} &= \sqrt{\Gamma_{3a\sigma}}(|0\rangle\langle 3_{a\sigma}| + \sum_{\sigma'} (|1_{b\sigma'}\rangle\langle 3_{a\sigma}1_{b\sigma'}| + |2_{b\sigma'}\rangle\langle 3_{a\sigma}2_{b\sigma'}| + |3_{b\sigma'}\rangle\langle 3_{a\sigma}3_{b\sigma'}|), \\ D_{3b\sigma} &= \sqrt{\Gamma_{3b\sigma}}(|0\rangle\langle 3_{b\sigma}| - \sum_{\sigma'} (|1_{a\sigma'}\rangle\langle 1_{a\sigma'}3_{b\sigma}| + |2_{a\sigma'}\rangle\langle 2_{a\sigma'}3_{b\sigma}| + |3_{a\sigma'}\rangle\langle 3_{a\sigma'}3_{b\sigma}|), \\ D_{1a\sigma}^\dagger &= \sqrt{\Gamma_{1a\sigma}}(|0\rangle\langle 1_{a\sigma}| + \sum_{\sigma'} (|1_{b\sigma'}\rangle\langle 1_{a\sigma}1_{b\sigma'}| + |2_{b\sigma'}\rangle\langle 1_{a\sigma}2_{b\sigma'}| + |3_{b\sigma'}\rangle\langle 1_{a\sigma}3_{b\sigma'}|), \\ D_{1b\sigma}^\dagger &= \sqrt{\Gamma_{1b\sigma}}(|0\rangle\langle 1_{b\sigma}| - \sum_{\sigma'} (|1_{a\sigma'}\rangle\langle 1_{a\sigma'}1_{b\sigma}| + |2_{a\sigma'}\rangle\langle 2_{a\sigma'}1_{b\sigma}| + |3_{a\sigma'}\rangle\langle 3_{a\sigma'}1_{b\sigma}|), \\ D_{2a\sigma}^\dagger &= \sqrt{\Gamma_{2a\sigma}}(|0\rangle\langle 2_{a\sigma}| + \sum_{\sigma'} (|1_{b\sigma'}\rangle\langle 2_{a\sigma}1_{b\sigma'}| + |2_{b\sigma'}\rangle\langle 2_{a\sigma}2_{b\sigma'}| + |3_{b\sigma'}\rangle\langle 2_{a\sigma}3_{b\sigma'}|), \\ D_{2b\sigma}^\dagger &= \sqrt{\Gamma_{2b\sigma}}(|0\rangle\langle 2_{b\sigma}| - \sum_{\sigma'} (|1_{a\sigma'}\rangle\langle 1_{a\sigma'}2_{b\sigma}| + |2_{a\sigma'}\rangle\langle 2_{a\sigma'}2_{b\sigma}| + |3_{a\sigma'}\rangle\langle 3_{a\sigma'}2_{b\sigma}|). \end{aligned} \quad (\text{B1})$$

In the following we set $\Gamma_{1A\sigma} = \Gamma_{1A}$, $\Gamma_{2A\sigma} = \Gamma_{2A}$ and $\Gamma_{3A\sigma} = \Gamma_{3A}$, $A = a, b$, $\sigma = \uparrow, \downarrow$. We have assumed energy independent rates $\Gamma_{iA\sigma} = 2\pi \sum_k |V_{\alpha k \sigma, A}|^2 \delta(\omega - \varepsilon_{\alpha k, A})$.

* E-mail: christina@itp.tu-berlin.de

¹ G. Alzetta, A. Gozzini, L. Moi, and G. Orriols, *Nuovo Cimento B* **36**, 5 (1976).

² E. Arimondo, and G. Orriols, *Lett. Nuovo Cimento* **17**, 333 (1976).

³ R. M. Whitley, and C. R. Stroud, *Phys. Rev. A* **14**, 1498

- (1976).
- ⁴ T. Brandes, and F. Renzoni, Phys. Rev. Lett. **85**, 4148 (2000).
 - ⁵ T. Brandes, Phys. Rep. **408**, 315 (2005).
 - ⁶ L. Faoro, J. Siewert, and R. Fazio, Phys. Rev. Lett. **90**, 028301 (2003).
 - ⁷ B. Michaelis, C. Emary, and C. W. J. Beenakker, Europhys. Lett. **73**, 677 (2006).
 - ⁸ C. W. Groth, B. Michaelis, and C. W. J. Beenakker, Phys. Rev. B **74**, 125315 (2006).
 - ⁹ C. Emary, Phys. Rev. B **76**, 245319 (2007).
 - ¹⁰ M. Busl, R. Sánchez, and G. Platero, Phys. Rev. B **81**, 121306 (2010).
 - ¹¹ M. Busl, R. Sánchez, and G. Platero, Physica E **42**(4), 830 (2010).
 - ¹² F. Domínguez, G. Platero, and S. Kohler, Chem. Phys. **375**, 284 (2010).
 - ¹³ M. Busl, and G. Platero, Journal of Physics: Condensed Matter **24**(15), 154001 (2012).
 - ¹⁴ I. Weymann, B. R. Buřka, and J. Barnaś, Phys. Rev. B **83**, 195302 (2011).
 - ¹⁵ F. Domínguez, S. Kohler, and G. Platero, Phys. Rev. B **83**, 235319 (2011).
 - ¹⁶ Z.-Z. Li, S.-H. Ouyang, C.-H. Lam, and J. Q. You, Europhys. Lett. **95**(4), 40003 (2011).
 - ¹⁷ C. Pörtl, C. Emary, and T. Brandes, Phys. Rev. B **80**, 115313 (2009).
 - ¹⁸ J.-p. Zhu, G.-x. Li, and Z. Ficek, Phys. Rev. A **85**, 033835 (2012).
 - ¹⁹ A more elaborate model for an exchange interaction is the Hubbard approximation (e.g.^{40,41}) on the spin dynamics, with a finite tunnel amplitude T_{ab} between TQD a and TQD b , the strength of the exchange interaction is $J_{ij} \sim T_{ab}^2/U_{AA}$, with U_{AA} being the charging energy for finding two electrons in one TQD. In our setup where we assume $T_{ab} \rightarrow 0$ and $U_{AA} \gg U_{ij}$, this would correspond to small exchange interaction.
 - ²⁰ P. Schijven, and O. Mülken, Phys. Rev. E **85**, 062102 (2012).
 - ²¹ S. A. Gurvitz, and Y. S. Prager, Phys. Rev. B **53**, 15932 (1996).
 - ²² S. A. Gurvitz, Phys. Rev. B **57**, 6602 (1998).
 - ²³ The set of equations given by Eq. (9) together with the normalization condition of the DS can be solve by symbolic computational software program (e.g. Mathematica). However these softwares may miss solutions and also find unphysical or uninteresting (e.g. with the condition $T_a = T_b = 0$) solutions. Such that each solution must be checked for its unques and it might be possible that further DSs exist that are not found.
 - ²⁴ L. S. Levitov, and G. B. Lesovik, JETP Lett. **58**(3), 230 (1993).
 - ²⁵ L. S. Levitov, H. Lee, and G. B. Lesovik, J. Math. Phys. **37**(10), 4845 (1996).
 - ²⁶ D. A. Bagrets, and Y. V. Nazarov, Phys. Rev. B **67**, 085316 (2003).
 - ²⁷ D. Marcos, C. Emary, T. Brandes, and R. Aguado, New J. Phys. **12**(12), 123009 (2010).
 - ²⁸ Directly at degenerate DSs the transport system is multistable. Hence, all DSs of the closed system are possible stationary states. The *real* stationary state, into which the transport system ends up, depends in this case on the initial conditions in which the system is prepared. But while approaching the DS, the systems runs into the mixture, where each of the four DSs is occupied with equal probability. This unique stationary state can also be generated by adding an infinitesimal amount of decoherence⁴ directly at the DS conditions to the transport Louvillian.
 - ²⁹ G. Burkard, D. Loss, and E. V. Sukhorukov, Phys. Rev. B **61**, R16303 (2000).
 - ³⁰ S. J. Freedman, and J. F. Clauser, Phys. Rev. Lett. **28**, 938 (1972).
 - ³¹ A. Aspect, P. Grangier, and G. Roger, Phys. Rev. Lett. **49**, 91 (1982).
 - ³² J. S. Bell, Physics **1**, 195 (1964).
 - ³³ D. P. DiVincenzo, Science **270**(5234), 255 (1995).
 - ³⁴ M. A. Nielsen, and I. L. Chuang, *Quantum computation and quantum information* (Cambridge University Press, New York, NY, USA, 2000).
 - ³⁵ C. H. Bennett, G. Brassard, C. Crépeau, R. Jozsa, A. Peres, and W. K. Wootters, Phys. Rev. Lett. **70**, 1895 (1993).
 - ³⁶ D. Bouwmeester, J.-W. Pan, K. Mattle, M. Eibl, H. Weinfurter, and A. Zeilinger, Nature **390**, 575 (1997).
 - ³⁷ A. K. Ekert, Phys. Rev. Lett. **67**, 661 (1991).
 - ³⁸ W. K. Wootters, Phys. Rev. Lett. **80**, 2245 (1998).
 - ³⁹ The original definition of the concurrence in Ref. [38] considers only the case where $\text{Tr}[\rho_{2Q}] = 1$. As we not only have a two particle sector of ρ_{spin} , but also an empty and a single particle sector, the trace of $\text{Tr}[\rho_{2Q}] < 1$ is in general smaller than one. Since the 'concurrence' for matrices with a different trace scales linearly with the value of the trace, we can also calculate C for a matrix with $\text{Tr}[\rho_{2Q}] < 1$ to measure the degree of entanglement. In the limit of large left tunnel rates and when the system is in the dark state the trace becomes unity anyway.
 - ⁴⁰ R. Hanson, L. P. Kouwenhoven, J. R. Petta, S. Tarucha, and L. M. K. Vandersypen, Rev. Mod. Phys. **79**, 1217 (2007).
 - ⁴¹ D. Loss, and D. P. DiVincenzo, Phys. Rev. A **57**, 120 (1998).